The Astrophysical Journal, 741:16 (13pp), 2011 November 1 doi:10.1088/0004-637X/741/1/16

MAGNETIC FIELD LINE RANDOM WALK FOR DISTURBED FLUX SURFACES: TRAPPING EFFECTS AND MULTIPLE ROUTES TO BOHM DIFFUSION

M. C. Ghilea[1,2], D. Ruffolo[1,2], P. Chuychai[2,3], W. Sonsrettee[1,2,4], A. Seripienlert[1,2,6], and W. H. Matthaeus[5]
[1] Department of Physics, Faculty of Science, Mahidol University, Bangkok 10400, Thailand; mghilea@gmail.com, scdjr@mahidol.ac.th, s_wirin@yahoo.com, achara.seri@gmail.com
[2] Thailand Center of Excellence in Physics, CHE, Ministry of Education, Bangkok 10400, Thailand
[3] School of Science, Mae Fah Luang University, Chiang Rai 57100, Thailand; p.chuychai@sci.mfu.ac.th
[4] Faculty of Engineering and Technology, Panyapiwat Institute of Management, Nonthaburi 11120, Thailand
[5] Bartol Research Institute and Department of Physics and Astronomy, University of Delaware, Newark, DE 19716, USA; yswhm@bartol.udel.edu
Received 2011 April 28; accepted 2011 July 25; published 2011 October 11

ABSTRACT

The magnetic field line random walk (FLRW) is important for the transport of energetic particles in many astrophysical situations. While all authors agree on the quasilinear diffusion of field lines for fluctuations that mainly vary parallel to a large-scale field, for the opposite case of fluctuations that mainly vary in the perpendicular directions, there has been an apparent conflict between concepts of Bohm diffusion and percolation/trapping effects. Here computer simulation and non-perturbative analytic techniques are used to re-examine the FLRW in magnetic turbulence with slab and two-dimensional (2D) components, in which 2D flux surfaces are disturbed by the slab fluctuations. Previous non-perturbative theories for $D_\perp$, based on Corrsin's hypothesis, have identified a slab contribution with quasilinear behavior and a 2D contribution due to Bohm diffusion with diffusive decorrelation (DD), combined in a quadratic formula. Here we present analytic theories for other routes to Bohm diffusion, with random ballistic decorrelation (RBD) either due to the 2D component itself (for a weak slab contribution) or the total fluctuation field (for a strong slab contribution), combined in a direct sum with the slab contribution. Computer simulations confirm the applicability of RBD routes for weak or strong slab contributions, while the DD route applies for a moderate slab contribution. For a very low slab contribution, interesting trapping effects are found, including a depressed diffusion coefficient and subdiffusive behavior. Thus quasilinear, Bohm, and trapping behaviors are all found in the same system, together with an overall viewpoint to explain these behaviors.

Key words: diffusion – magnetic fields – turbulence

1. INTRODUCTION

Turbulent magnetic fields are omnipresent in astrophysical plasmas, and the motion of energetic charged particles basically follows the magnetic field. Thus, the random walk of magnetic field lines in space is directly relevant to the transport of such particles perpendicular to the large-scale magnetic field (e.g., Jokipii 1966; Urch 1977; Matthaeus et al. 2003; Ruffolo et al. 2008). Early descriptions of the field line random walk (FLRW) in magnetic turbulence used a quasilinear theory (Jokipii 1966; Jokipii & Parker 1968), which is now known to apply to fluctuations that vary mainly along a large-scale field, such as parallel-propagating Alfvén waves, or for which the Kubo number (see Kubo 1963) is much less than 1 (if it exists). In this case, the FLRW initially undergoes free streaming until traveling over the order of the mean free path, after which the FLRW becomes diffusive. If z is the coordinate along a large-scale magnetic field of magnitude B_0, the diffusion along the perpendicular coordinates can be characterized by a diffusion coefficient $D_\perp \equiv \langle \Delta x^2 + \Delta y^2 \rangle / (4\Delta z)$. Quasilinear theory yields $D_\perp \propto (b/B_0)^2$, where b is the root-mean-squared magnetic fluctuation.

For transverse fluctuations that mainly vary in directions perpendicular to the large-scale field (e.g., at a high Kubo number $R \gg 1$), as are expected to result from the magnetohydrodynamic (MHD) interactions of counter-propagating Alfvén waves (Shebalin et al. 1983), there has been disagreement about the form of the diffusion coefficient. For the related problem of two-dimensional (2D) hydrodynamic turbulence, Salu & Montgomery (1977) obtained Bohm diffusion, which in this context means the dependence $D_\perp \propto b/B_0$. They described a process based on diffusive decorrelation (DD), assuming Corrsin's hypothesis (Corrsin 1959). Kadomtsev & Pogutse (1979) also inferred Bohm diffusion, based on a dimensional argument related to what (in the present work) we term random ballistic decorrelation (RBD). For a two-component 2D+slab model of turbulence (to be described shortly) in which the 2D component dominates, the non-perturbative theory of Matthaeus et al. (1995) predicted Bohm diffusion using the DD approach, which was confirmed in computer simulations by Gray et al. (1996).

On the other hand, for a related problem (2D hydrodynamic turbulence with slowly varying fields), Gruzinov et al. (1990) proposed a theory involving percolation, which was taken by Isichenko (1991b) to apply to the FLRW for a high Kubo number and weak fluctuations. In this theory, $D_\perp \approx (b/B_0)R^{-3/10}$, where the Kubo number is $R \equiv (b/B_0)(\ell_c/\ell_\perp)$, and ℓ_c and $\ell_\perp$ are the parallel and perpendicular correlation lengths, respectively. There is some computational confirmation for the FLRW and analogous problems (e.g., Ottaviani 1992; Reuss & Misguich 1996; Hauff et al. 2010). Considerations related to percolation have also been referred to as trapping effects (e.g., Ottaviani 1992; Vlad et al. 1998; Neuer & Spatschek 2006; Negrea et al. 2007), a term that is broader than percolation. Additional theoretical techniques include the decorrelation trajectory method and A-Langevin equations (Vlad et al. 1998; Neuer & Spatschek 2006). Advocates of percolation models frequently refer to Bohm diffusion as incorrect, though some of their arguments were perhaps meant to apply to a limit of extremely high R and an FLRW strongly dominated by 2D structures.

[6] Now at Dacon Inspection Services Co., Ltd., Rayong 21130, Thailand.

Here we re-examine the nature of the FLRW in the context of the two-component 2D+slab model of magnetic turbulence. This model describes magnetostatic fluctuations as a sum of a slab component that only varies along the large-scale field, which could be physically due to a spectrum of Alfvénic fluctuations, and a 2D component that only varies in the perpendicular directions, which could be due to a perpendicular cascade from interacting waves (Shebalin et al. 1983). The model was motivated by observations of a similar dichotomy in fluctuations of the interplanetary magnetic field (Matthaeus et al. 1990; Dasso et al. 2005; Osman & Horbury 2007; Weygand et al. 2009), and has proven useful in describing turbulence in the typical solar wind (Bieber et al. 1996), a magnetic cloud (Leamon et al. 1998), and a structure of high Alfvén speed (Smith et al. 2001, 2004), as well as in explaining a wide range of particle transport observations (Bieber et al. 1994, 2004; Shalchi et al. 2006). The 2D+slab model is a simplification that facilitates analytic calculations and computer simulations. The 2D component has flux surfaces that project onto equipotential contours in the x–y plane (Figure 1(a)), but these flux surfaces are disturbed upon the addition of slab fluctuations (Figure 1(b)); see also Figures 1 and 2 of Matthaeus et al. (1995). That work predicted that the FLRW would exhibit quasilinear diffusion when the slab component dominates and Bohm diffusion when the 2D component dominates, which was confirmed by Gray et al. (1996) for a wide range of parameters. However, as part of a survey of particle transport properties, Ruffolo et al. (2008) performed a simulation run for a very low slab energy fraction, $f_s = 0.01$, and an unusual FLRW was found: free streaming was followed by transient subdiffusion and lower asymptotic diffusion than expected. (Note that Ottaviani (1992) previously found transient subdiffusion followed by asymptotic diffusion at high Kubo number for a different fluctuation model in a transport problem analogous to the FLRW.) Subdiffusion seems to indicate trapping effects, in which field lines are temporarily trapped in topological structures of the 2D turbulence (see Ruffolo et al. 2003; Zimbardo et al. 2004; Chuychai et al. 2007; Seripienlert et al. 2010).

In the present work, we confirm that the slab contribution to the FLRW is quasilinear diffusion, and we find a variety of behaviors for the 2D contribution. For this contribution, in addition to the previously known route to Bohm diffusion (Matthaeus et al. 1995), described by Corrsin's hypothesis with DD, we find additional routes to Bohm diffusion involving RBD. Each type of Bohm diffusion can provide a useful description over a different parameter range. For very low slab contributions, the disturbance of the 2D flux surfaces is so weak that trapping effects cause a reduction in the diffusion coefficient, as the assumptions underlying the derivations of Bohm diffusion become less accurate, and at the lowest slab fractions we can confirm subdiffusive behavior (which makes it difficult to measure diffusion coefficients for comparison with percolation theory). Thus, we have identified a system in which the FLRW has contributions from quasilinear and Bohm diffusion over most of the parameter range examined, but trapping effects are strong in the limit where the FLRW is largely constrained to only weakly disturbed 2D flux surfaces, reconciling many of the claims of previous studies.

2. MULTIPLE ROUTES TO BOHM DIFFUSION

2.1. Magnetic Field Model

We examine the random walk of magnetic field lines and the perpendicular diffusion coefficients for the case of the two-component 2D+slab turbulence model, in which the magnetic field is expressed as

$$\mathbf{B} = B_0\hat{\mathbf{z}} + \mathbf{b}(x, y, z), \tag{1}$$

where $B_0\hat{\mathbf{z}}$ is a constant mean (large-scale) field. The fluctuation $\boldsymbol{b}$ is transverse, so that $\mathbf{b} \perp \hat{\mathbf{z}}$, and $\mathbf{b}$ is separable into two components, a "slab" component that depends only on the z-coordinate and a "2D" component that depends only on the x- and y-coordinates:

$$\mathbf{b}(x, y, z) = \mathbf{b}^{\rm slab}(z) + \mathbf{b}^{\rm 2D}(x, y). \tag{2}$$

Because we must have $\nabla \cdot \mathbf{B} = 0$ and by construction $\nabla \cdot B_0\hat{\mathbf{z}} = \nabla \cdot \mathbf{b}^{\rm slab}(z) = 0$, therefore $\nabla \cdot \mathbf{b}^{\rm 2D} = 0$, which is satisfied when $\mathbf{b}^{\rm 2D} = \nabla \times [a(x, y)\hat{\mathbf{z}}]$ for a scalar potential function $a(x, y)$. For pure 2D fluctuations, the magnetic field lines exactly follow 2D flux surfaces (Figure 1(a)) defined by contours of constant potential (also shown in Figure 2), but the addition of the slab component allows field lines to diffuse away from the 2D flux surfaces (Figures 1(b) and 2).

For a magnetic field model organized around a mean field $\mathbf{B}_0$, the two-component model includes elements of a traditional slab model (Jokipii 1966) as well as a 2D rendition of the highly oblique wavevectors that are favored by anisotropic spectral transfer (Shebalin et al. 1983). The motivation for this model is mainly to provide both analytical and computational simplicity—note that for N_z slab modes and $N_x \times N_y$ 2D modes, the two-component model involves many fewer total degrees of freedom than would a full $N_x \times N_y \times N_z$ three-dimensional model. However the model is in fact three-dimensional, in that both the mean square and local gradients are in general oblique, and a test particle in any region of space will encounter local variations in arbitrary directions. While the model is clearly not complete, it provides an approximate separation into perpendicular and parallel-propagating transverse "Alfven modes." The parallel variance modes are ignored in this model (see however Matthaeus & Ghosh 1999), thus discarding the "fast mode" contribution (e.g., Carbone et al. 1995) which is thought in any case to evolve somewhat independently (Cho & Lazarian 2002) and to represent a small ingredient in solar wind turbulence (Belcher & Davis 1971).

Note that we use the symbol b^2 as a shorthand for the fluctuation energy $\langle b^2 \rangle$, either for total fluctuations or a single component, and thus b refers to the root-mean-squared fluctuation $\sqrt{\langle b^2 \rangle}$. The slab and 2D contributions are taken to be statistically independent, so $b^2 = b^2_{\rm slab} + b^2_{\rm 2D}$. In the present work we assume axisymmetry, with statistical rotational symmetry around the mean field direction, $\hat{\mathbf{z}}$, so that fluctuations are statistically identical in the x- and y-directions (the assumption of axisymmetry was relaxed in some FLRW studies; see Pommois et al. 2001; Ruffolo et al. 2006; Weinhorst et al. 2008). Axisymmetry implies statistically identical properties of field line trajectories along x and y.

Because the fluctuations are transverse, a field line never backtracks in z, and we can use this coordinate to uniquely specify a location along the field line. Then the field line trajectory is specified by $x(z)$ and $y(z)$, determined by

$$\frac{dx}{dz} = \frac{b_x(x, y, z)}{B_0} \qquad \frac{dy}{dz} = \frac{b_y(x, y, z)}{B_0}. \tag{3}$$

2.2. Concepts

Before undertaking the full mathematical derivation of the asymptotic diffusion coefficient, let us introduce the key

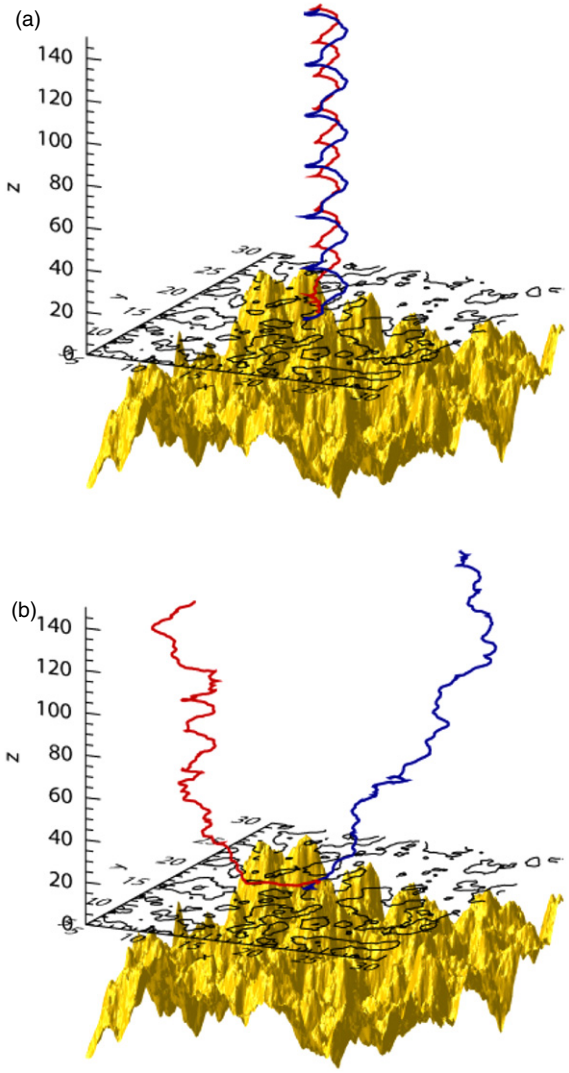

Figure 1. Magnetic field line trajectories (red and blue lines) in a representation of 2D turbulence, $\mathbf{b}^{2D}(x, y)$, added to a mean field $B_0\hat{\mathbf{z}}$, (a) without and (b) with a component of slab turbulence, $\mathbf{b}^{slab}(z)$. The surface plot at the bottom shows the 2D potential function $a(x, y)$, and equipotential contours are indicated for a certain value of a (black lines). In the absence of a slab component, the field lines are trapped on equipotential flux surfaces, which project onto contours of constant a. With 20% of the fluctuation energy in a slab component, the flux surfaces are disturbed and the field lines asymptotically diffuse in the x- and y-directions with a combination of quasilinear diffusion due to the slab component and Bohm diffusion associated with the 2D component.

concepts in terms of simple, order-of-magnitude relations. For diffusive behavior associated with axisymmetric fluctuations, we have

$$\langle \Delta x^2 \rangle = \langle \Delta y^2 \rangle = 2D_\perp \Delta z \tag{4}$$

$$D_\perp \sim \langle (dx/dz)^2 \rangle \, \ell \sim \frac{\langle b_x^2 \rangle}{B_0^2} \, \ell \tag{5}$$

for a "mean free distance" ℓ in the z-direction (Ruffolo et al. 2004).

The prescription for ℓ depends on what process determines the decorrelation of b_x. For slab fluctuations, in which b_x depends only on z, the decorrelation is due to the trajectory of the field line along z, according to the mean field $B_0\hat{\mathbf{z}}$. Then, it is natural

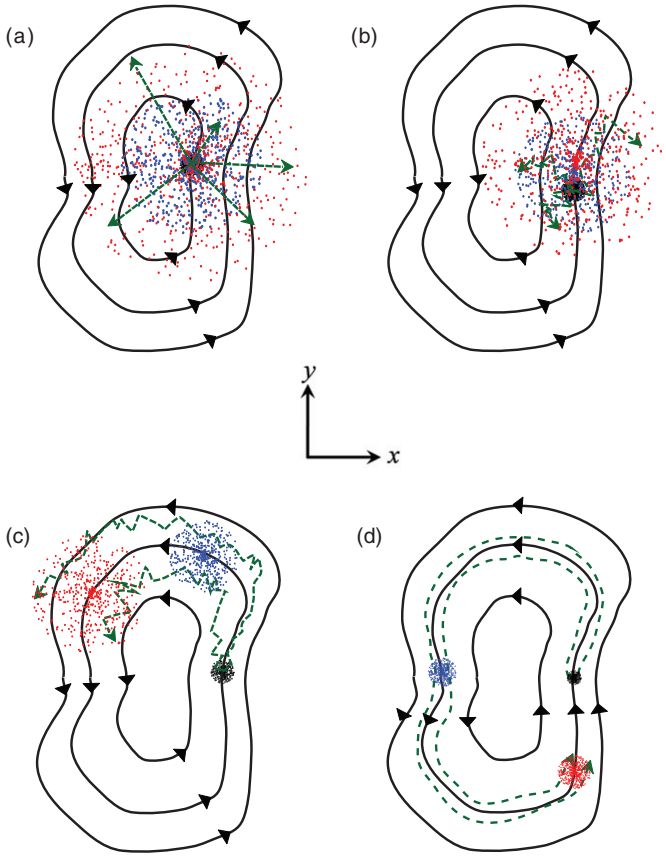

Figure 2. Illustration of four regimes of magnetic field line random walks (green dashed lines) in 2D+slab turbulence, for which different processes govern the Lagrangian decorrelation of the 2D field. The 2D field follows equipotential contours (black lines) while the slab field varies randomly with z. Colored dots illustrate the distribution of field line locations for an ensemble of slab fields at varying distance z from a common starting point (at increasing z for black, blue, and red points, respectively). (a) For a strong slab contribution, there is random ballistic decorrelation (RBD) of the 2D field due to nearly straight field line trajectories (dominated by slab fluctuations). We call this RBD/2D+slab because both components contribute to the ballistic trajectories. (b) For a moderate slab contribution, there is diffusive decorrelation (DD) of the 2D field due to diffusion (again dominated by slab fluctuations). (c) For a weak slab contribution, there is RBD due to the 2D field itself, called RBD/2D. Note that panels (a)–(c) all represent routes to Bohm diffusion for the 2D contribution. (d) For a very weak slab contribution, field lines remain trapped along 2D flux surfaces for long distances, with "memory effects," and in some cases the field line random walk is subdiffusive.

for ℓ to be of the order of the correlation length ℓ_c:

$$D_\perp^{slab} \sim \frac{1}{2} \frac{b_{slab}^2}{B_0^2} \, \ell_c = \frac{f_s}{2} \frac{b^2}{B_0^2} \, \ell_c, \tag{6}$$

where $f_s \equiv b_{slab}^2/b^2$ is the slab fraction of the fluctuation energy. (Note that for axisymmetric turbulence, $b^2 = \langle b^2 \rangle = 2\langle b_x^2 \rangle$, either for the total fluctuation field or for either component.) In fact, Equation (6) is an equality, to be derived in the next section. When the diffusion coefficient depends on the square of the fluctuation amplitude, as in this case, we refer to quasilinear diffusion.

For 2D fluctuations, the decorrelation instead occurs when the x–y displacement is on the order of a perpendicular length scale of the turbulence. Let us call the scale $\ell_\perp$ and reserve its precise specification for the derivation in Section 2.3. Previous detailed derivations (Salu & Montgomery 1977; Matthaeus et al. 1995) have assumed DD with the asymptotic diffusion coefficient.

Setting $\langle \Delta x^2 \rangle$ to $\ell_\perp^2$ in Equation (4) yields

$$\ell \sim \frac{\ell_\perp^2}{2D_\perp}, \tag{7}$$

so the 2D contribution to the diffusion coefficient is

$$D_\perp - D_\perp^{\rm slab} \sim \frac{1}{2}\frac{b_{\rm 2D}^2}{B_0^2}\frac{\ell_\perp^2}{2D_\perp}. \tag{8}$$

For the case where the slab contribution is negligible, we use the symbol $D_\perp^{\rm 2D}$:

$$D_\perp^{\rm 2D} \sim \frac{1}{2}\frac{b_{\rm 2D}}{B_0}\ell_\perp. \tag{9}$$

In a more general context, $b_{\rm 2D} = \sqrt{1-f_s}\,b$, so

$$D_\perp^{\rm 2D} \sim \frac{\sqrt{1-f_s}}{2}\frac{b}{B_0}\ell_\perp. \tag{10}$$

When the diffusion coefficient depends on the first power of the fluctuation amplitude, we refer to Bohm diffusion, and this line of reasoning comprises one route to Bohm diffusion.

Then Equation (8) can be written as

$$D_\perp - D_\perp^{\rm slab} = \frac{(D_\perp^{\rm 2D})^2}{2D_\perp}, \tag{11}$$

which has the solution (Matthaeus et al. 1995)

$$D_\perp = \frac{D_\perp^{\rm slab}}{2} + \sqrt{\left(\frac{D_\perp^{\rm slab}}{2}\right)^2 + (D_\perp^{\rm 2D})^2}, \tag{12}$$

so the slab and 2D terms combine in a "quadratic" fashion due to the dependence on $D_\perp$ on the right-hand side of Equation (11).

As an aside, consider the scaling of the field line Equations (3) by the bendover scales of the slab and 2D turbulence, i.e., λ and $\lambda_\perp$. Using $\mathbf{x}'_\perp = \mathbf{x}_\perp/\lambda_\perp$, where $\mathbf{x}_\perp = (x, y)$, and $z' = z/\lambda$, we obtain

$$\frac{d\mathbf{x}'_\perp}{dz'} = \frac{\mathbf{b}}{B_0}\frac{\lambda}{\lambda_\perp}. \tag{13}$$

Now consider the scaled fluctuation amplitude

$$r \equiv \frac{b}{B_0}\frac{\lambda}{\lambda_\perp}. \tag{14}$$

A similar quantity was considered by Ruffolo et al. (2004). For a given type of turbulence, i.e., a given f_s, the scaled diffusion coefficient $D' = D(\lambda/\lambda_\perp^2)$ should depend only on r. Thus we use r, along with f_s, as a control parameter when reporting results for the field line diffusion coefficient (see Section 3). Note also that for an intermediate value of f_s, assuming the correlation scales ℓ_c and $\ell_\perp$ to be of the same order of magnitude as the spectral bendover scales λ and $\lambda_\perp$, respectively, we have

$$r \sim \frac{D_\perp^{\rm slab}}{D_\perp^{\rm 2D}}, \tag{15}$$

so r also characterizes the relative contributions of the slab and 2D components.

Although r appears similar to the widely used Kubo number, and they are based on the same scaling, they are physically distinct. For the FLRW, the Kubo number is typically defined as $R = (b/B_0)(l_c/l_\perp)$, where l_c and $l_\perp$ are correlation lengths of the *total* magnetic field parallel and perpendicular to the mean magnetic field, respectively. Typically, this quantity is used for one-component anisotropic turbulence. However, for two-component 2D+slab turbulence the Kubo number is indeterminate: l_c is infinite (because the 2D component is independent of z) and $l_\perp$ is infinite (because the slab component is independent of x and y). Another important difference is that $r \gg 1$ implies quasilinear behavior—which is characteristic of $R \ll 1$ for one-component turbulence (Isichenko 1991a).

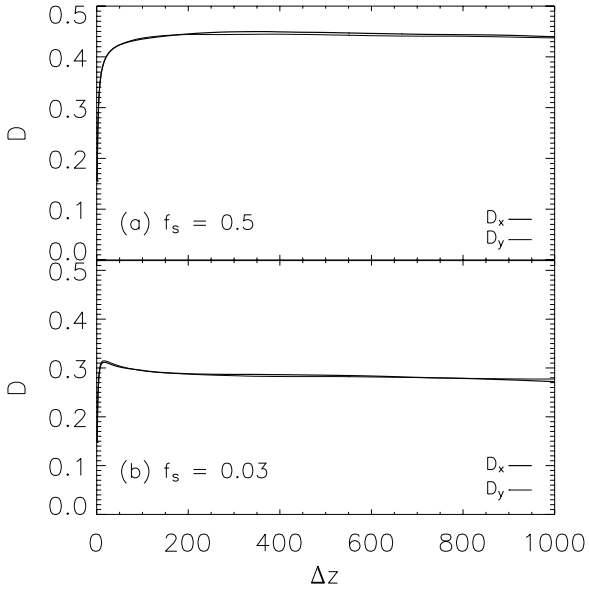

Figure 3. Examples of computer simulation results for magnetic field line diffusion coefficients $D_x = \langle \Delta x^2 \rangle/(2\Delta z)$ and $D_y = \langle \Delta y^2 \rangle/(2\Delta z)$ as a function of Δz for $r = (b/B_0)(\lambda_\parallel/\lambda_\perp) = 1$ and a slab fraction of (a) $f_s = 0.5$ and (b) $f_s = 0.03$. The turbulence is axisymmetric, so D_x and D_y should differ only through statistical fluctuations. In each case, D_x and D_y rise rapidly at low Δz because of free streaming, before the full development of a random walk. At large Δz, they gradually decrease due to a numerical periodicity effect. For panel (a), D_x and D_y reach nearly constant values, indicating asymptotic diffusion. For panel (b), the diffusion coefficients peak and then decrease, indicating a subdiffusive field line random walk. Because of the periodicity effect, it is unclear whether the asymptotic behavior is subdiffusive or diffusive.

Returning to the concepts of diffusion, the assumption of diffusion in Equation (7) seems natural, given that we are performing a calculation of diffusive behavior. However, a turbulent FLRW typically exhibits free streaming at small displacements Δz and asymptotic diffusion at larger displacements (Figure 3(a)). Then, the question arises as to whether the mean free path ℓ in the z-direction—which relates to the initial decorrelation of the random walk—is determined by the formula for asymptotic diffusion or by the free-streaming behavior at smaller displacements.

Actually, the most common assumption in random walk theory is that individual "steps" are ballistic (not yet diffusive), either as straight-line trajectories (free streaming) or motion according to a background force, until a "collision" starts to decorrelate the random walk. If the decorrelation is eventually complete, after a few correlation lengths, then at that later stage the random walk achieves asymptotic diffusion. Accordingly, in the present work, we consider alternative routes to Bohm diffusion with random ballistic diffusion (RBD) in the initial free-streaming regime, instead of DD.

Either RBD or DD may be appropriate to describe the (Bohm) 2D contribution to the diffusion, depending on the strength of the

quasilinear slab contribution. To illustrate this, Figure 2 shows nested flux surfaces of the 2D field, i.e., equipotential contours of the potential function $a(x, y)$, and colored points schematically indicate the spread of field lines for that 2D field plus an ensemble of slab fields; each color represents the distribution at a different Δz. We identify four regimes of behavior.

1. For the case of a strong slab contribution, Figure 2(a) illustrates that a field line can rapidly move in a random direction due to the slab field, and when the slab field is sufficiently strong, motion during the free-streaming regime is sufficient to decorrelate (e.g., change the direction of) the 2D field. Thus, the mean free path is specified by an ensemble of straight-line trajectories (represented by expanding "clouds" of field line locations in Figure 2(a)), until the x (or y) displacement is of order $\ell_\perp$:

$$\ell \sim \frac{\ell_\perp}{(dx/dz)_{\rm rms}} = \frac{B_0}{\sqrt{\langle b_x^2\rangle}}\,\ell_\perp, \tag{16}$$

where $\langle b_x^2\rangle$ includes both slab and 2D contributions. We therefore use the shorthand "RBD/2D+slab" to refer to this route of RBD. Then we obtain another form of Bohm diffusion:

$$D_\perp - D_\perp^{\rm slab} = D_\perp^{\rm 2D} \sim \frac{1}{2}\frac{b_{\rm 2D}^2}{B_0^2}\,\ell = \frac{1-f_s}{\sqrt{2}}\frac{b}{B_0}\,\ell_\perp \tag{17}$$

$$D_\perp = D_\perp^{\rm slab} + D_\perp^{\rm 2D}. \tag{18}$$

Kadomtsev & Pogutse (1979) presented a similar qualitative argument for Bohm diffusion at high Kubo number. Note that compared with the DD route to Bohm diffusion, in this RBD route the dependence on f_s is different, the specification of $\ell_\perp$ is different (see Section 2.3), and the slab and 2D contributions combine in a direct sum.
2. For a moderate slab contribution (Figure 2(b)), it is possible that slab turbulence in the free-streaming regime is insufficient to carry magnetic field lines over a scale $\ell_\perp$ (the x–y distance over which $\mathbf{b}_{\rm 2D}$ changes), but in the diffusive regime the slab contribution does decorrelate the random walk more rapidly than the 2D contribution to the trajectory. In this case, it is appropriate to use DD and Equations (10) and (12) as derived by Matthaeus et al. (1995).
3. For a weak slab contribution (Figure 2(c)), the slab fluctuations do not significantly contribute to the decorrelation of the 2D fluctuations. Therefore, the 2D fluctuations decorrelate due to the initial 2D ballistic contribution to the field line trajectory, and after the decorrelation the 2D fluctuations contribute to a diffusive random walk, provided there are sufficient slab fluctuations to escape from nested 2D flux structures. Assuming the slab contribution to be diffusive (and weak), we use a model of RBD due to the 2D component alone, for which we use the shorthand "RBD/2D":

$$\ell \sim \frac{B_0}{\sqrt{\langle b_x^2\rangle_{\rm 2D}}}\,\ell_\perp, \tag{19}$$

$$D_\perp - D_\perp^{\rm slab} = D_\perp^{\rm 2D} \sim \sqrt{\frac{1-f_s}{2}}\frac{b}{B_0}\,\ell_\perp \tag{20}$$

$$D_\perp = D_\perp^{\rm slab} + D_\perp^{\rm 2D}. \tag{21}$$

The formula for $D_\perp^{\rm 2D}$ appears similar to that for DD (for a moderate slab contribution) but $\ell_\perp$ is different and the slab and 2D contributions combine in a direct sum.
4. For a very weak slab contribution (Figure 2(d)), there is very little disturbance of 2D flux surfaces, and a field line experiences temporary topological trapping in a set of nested flux surfaces (Ruffolo et al. 2003). This phenomenon underlies observed "dropouts" in solar energetic particle fluxes (Mazur et al. 2000; Gosling et al. 2004), which are attributed to complex, intermittent patterns of field line connection from a compact particle source at the Sun (an impulsive solar flare site) to a detector near Earth (Giacalone et al. 2000; Ruffolo et al. 2003; Zimbardo et al. 2004; Pommois et al. 2005). The key mechanism for field lines (or particles) to escape from a set of nested 2D flux surfaces is the slab contribution to diffusion, but such diffusive escape is suppressed across a flux surface where the mean squared 2D field is strong and/or the flux surface is convoluted (Chuychai et al. 2005, 2007; Tooprakai et al. 2007; Seripienlert et al. 2010).

   Previous computer simulations have shown that in some cases, corresponding to Regime 3 above, temporary topological trapping and suppressed diffusive escape apply to subsets of field lines (with "conditional statistics" that depend on the initial conditions) but have little effect on the ensemble average statistics. In the context of the 2D+slab model, to see a substantial reduction in the ensemble average diffusion coefficient requires a very weak slab contribution and hence was noticed only recently (Ruffolo et al. 2008). Subdiffusion has also been found in computer simulations (Figure 3(b); see also Ruffolo et al. 2008). Such effects represent a breakdown in our theories of Bohm diffusion, presumably because for a very weak slab contribution, a field line that repeatedly follows similar trajectories around a 2D flux surface (approaching the pure 2D case shown in Figure 1(a)) has a longer-term "memory." Such behavior for other models of turbulent fluctuations has been addressed by the percolation theories of Gruzinov et al. (1990) and Isichenko (1991b), computer simulations by Ottaviani (1992), and later work in the literature.

All four regimes of behavior can be distinguished in terms of the dependence of $D_\perp$ on r and f_s, and are identified in our computer simulation results (Section 3).

2.3. Analytic Theory

For the first three of these four regimes of behavior, we have developed non-perturbative analytic theories for the asymptotic diffusion coefficients, which are consistent with the dependences worked out in the previous section. The calculations here initially follow Matthaeus et al. (1995) and Ruffolo et al. (2004). For transverse fluctuations, the trajectory of a magnetic field line satisfies Equations (3). Then the change in, say, the x-coordinate over a distance Δz along the mean field is

$$\Delta x \equiv x(\Delta z) - x(0) = \frac{1}{B_0}\int_0^{\Delta z} b_x[\mathbf{x}_\perp(z'), z']dz', \tag{22}$$

where $\mathbf{x}_\perp = (x, y)$ is a (random) field line trajectory. The ensemble average of $(\Delta x)^2$ can be expressed by

$$\langle \Delta x^2\rangle = \frac{1}{B_0^2}\int_0^{\Delta z}\int_0^{\Delta z}\langle b_x[\mathbf{x}_\perp(z'), z']b_x[\mathbf{x}_\perp(z''), z'']\rangle dz'dz''. \tag{23}$$

With the assumption of statistical homogeneity, one can write

$$\langle \Delta x^2 \rangle = \frac{1}{B_0^2} \int_0^{\Delta z} \left[\int_{-z'}^{\Delta z - z'} \langle b_x(0,0) b_x[\mathbf{\Delta x}'_\perp(z), z] \rangle dz \right] dz', \tag{24}$$

where $\mathbf{\Delta x}'_\perp \equiv \mathbf{x}_\perp(z'') - \mathbf{x}_\perp(z')$ and $z \equiv z'' - z'$ for locations along a field line trajectory. Since we aim to address asymptotic diffusion for large Δz, which occurs when the correlation vanishes after a very long distance, we can extend the limits of the z integration to $\pm\infty$, in which case the z' integration is trivial. Then we obtain

$$\langle \Delta x^2 \rangle = \frac{\Delta z}{B_0^2} \int_{-\infty}^{\infty} \langle b_x(0,0) b_x[\mathbf{\Delta x}'_\perp(z), z] \rangle dz, \tag{25}$$

which is related to the Taylor–Green–Kubo formula for the diffusion coefficient (Taylor 1920; Green 1951; Kubo 1957).

As an aside, we note that even before making any special assumptions, such as Corrsin's hypothesis, we can make general statements about the diffusion coefficient for 2D+slab turbulence. Given Equation (2) and the statistical independence of slab and 2D fields, and using $D_\perp = \langle \Delta x^2 \rangle / (2\Delta z)$, we have

$$D_\perp = \frac{1}{B_0^2} \int_0^{\infty} \left\langle b_x^{\rm slab}(0) b_x^{\rm slab}(z) \right\rangle + \left\langle b_x^{\rm 2D}(0) b_x^{\rm 2D}[\mathbf{\Delta x}'_\perp(z)] \right\rangle dz. \tag{26}$$

We refer to the terms on the right-hand side as the slab contribution and 2D contribution, respectively. We note that the slab contribution depends on the slab field alone; however, the function $\mathbf{\Delta x}'_\perp(z)$ for a given field line involves both 2D and slab fields, so both of them influence the 2D contribution to the diffusion coefficient.

Next, our first key assumption is Corrsin's independence hypothesis (Corrsin 1959). This assumption relates the Lagrangian correlation function in Equation (25) to the Eulerian correlation function, $R_{xx} \equiv \langle b_x(0,0) b_x(\mathbf{x}_\perp, z) \rangle$, averaged using the conditional probability $P(\mathbf{x}_\perp|z)$ of finding a displacement $\mathbf{x}_\perp$ after a distance z:

$$\langle b_x(0,0) b_x[\mathbf{\Delta x}'_\perp(z), z] \rangle = \int R_{xx}(\mathbf{x}_\perp, z) P(\mathbf{x}_\perp|z) d\mathbf{x}_\perp.$$

Corrsin's hypothesis is a good approximation if (but not only if) one can assume independence between the distribution (for fixed $\Delta z'$) of the Eulerian product $b_x(0,0) b_x(\mathbf{x}_\perp, z)$ and the probability distribution $P(\mathbf{x}_\perp|z)$. For sufficiently long $\Delta z'$ along a random walk with no "memory" of its prior path, one can safely assume such independence. This can be expected to be valid for distances where asymptotic diffusion applies in the first three of the four regimes described in Section 2.2. However, in the fourth regime, with a very weak slab contribution and strong trapping that results in a quasi-periodic trajectory along 2D flux surfaces (Figure 2(d)), the random walk has a "memory" in the sense of repeating the same path many times, and the validity of the hypothesis is unclear. In Section 4, we will further discuss the validity of Corrsin's hypothesis and other assumptions in our theories.

At this point, we employ the 2D+slab model, with statistically independent 2D and slab components, so that

$$R_{xx}(\mathbf{x}_\perp, z) = R_{xx}^{\rm slab}(z) + R_{xx}^{\rm 2D}(\mathbf{x}_\perp). \tag{27}$$

Using only the slab portion $R_{xx}^{\rm slab}$, we can find the slab contribution to the mean squared displacement:

$$\langle \Delta x^2 \rangle_{\rm slab} = \frac{\Delta z}{B_0^2} \int_{-\infty}^{\infty} R_{xx}^{\rm slab}(z) dz. \tag{28}$$

Note that the conditional probabilities play no role and simply integrate to 1, because the slab turbulence is independent of the displacement $\mathbf{x}_\perp$. Employing the power spectrum P_{xx}, the Fourier transform of R_{xx}, we obtain

$$D_\perp^{\rm slab} = \sqrt{\frac{\pi}{2}} \frac{P_{xx}^{\rm slab}(0)}{B_0^2} = \frac{\langle b_x^2 \rangle^{\rm slab}}{B_0^2} \ell_c \tag{29}$$

for the slab correlation length ℓ_c, as originally derived by Jokipii & Parker (1968). In terms of the slab fraction, f_s, we have

$$D_\perp^{\rm slab} = \frac{f_s}{2} \frac{b^2}{B_0^2} \ell_c. \tag{30}$$

This expression, with a dependence on the square of the fluctuation amplitude, is called quasilinear because it would result from a quasilinear approximation in which an unperturbed path (e.g., the mean field line) is used to estimate the perturbations due to fluctuations. However, in this case the slab turbulence is strictly independent of the path (depending only on the z-coordinate), so the quasilinear result is not an approximation and is non-perturbative, i.e., not restricted to a small fluctuation amplitude.

Now turning to the calculation of $\langle \Delta x^2 \rangle_{\rm 2D}$, we make a second key assumption that the conditional probability is Gaussian and independent for displacements in the x- and y-directions:

$$\begin{aligned} P(\mathbf{x}_\perp|z) &= P(x|z) P(y|z) \\ P(x|z) &= \frac{1}{\sqrt{2\pi\sigma_x^2}} \exp\left(-\frac{x^2}{2\sigma_x^2}\right) \\ P(y|z) &= \frac{1}{\sqrt{2\pi\sigma_y^2}} \exp\left(-\frac{y^2}{2\sigma_y^2}\right). \end{aligned} \tag{31}$$

In this work we consider the axisymmetric case, so $\sigma_x^2 = \sigma_y^2$.

The third key assumption specifies σ_x^2 and σ_y^2 as a function of z. At this point, previous work has assumed *diffusive spreading* of field lines over the distance scales relevant to decorrelation of the random walk. That is,

$$\sigma_x^2 = \sigma_y^2 = 2 D_\perp z. \tag{32}$$

We call this DD as suggested in Section 2.2. This leads to the result originally derived by Matthaeus et al. (1995),

$$D_\perp^{\rm 2D} = \frac{\tilde{\lambda}}{\sqrt{2}} \frac{b_{\rm 2D}}{B_0} \tag{33}$$

$$D_\perp = \frac{D_\perp^{\rm slab}}{2} + \sqrt{\left(\frac{D_\perp^{\rm slab}}{2}\right)^2 + \left(D_\perp^{\rm 2D}\right)^2}, \tag{34}$$

where we use a slightly different definition of the "ultrascale" $\tilde{\lambda}$ (see also Ruffolo et al. 2004; Matthaeus et al. 2007):

$$\tilde{\lambda} \equiv \sqrt{\frac{\langle a^2 \rangle}{b_{\rm 2D}^2}}, \tag{35}$$

in terms of the mean squared potential function $a(x, y)$ (see Section 2.1).

As discussed in Section 2.2, we expect such Bohm diffusion for $D_\perp^{2D}$, based on DD (Equation (32)), to apply for moderately strong slab turbulence (the second regime). For a slab contribution that is strong or weak (but not very weak), we instead expect RBD, which provides other routes to Bohm diffusion. Starting with the first regime, for a strong slab contribution, the derivation proceeds as follows.

In place of the assumption of diffusive spreading (Equation (32)), which corresponds to Equation (18) of Ruffolo et al. (2004), let us consider the case where there is *ballistic spreading* in random directions over the distance scales relevant to decorrelation of the random walk. We identify these random trajectories with the one-point statistics of the magnetic field, consisting of the mean field plus axisymmetric fluctuations. For this ensemble of straight-line (ballistic) trajectories (see Figure 2(a)), we use

$$\sigma_x^2 = \sigma_y^2 = \frac{\langle b_x^2 \rangle}{B_0^2} z^2. \tag{36}$$

For this regime, $\langle b_x^2 \rangle$ refers to the sum of 2D and slab components, because both contribute to the RBD; thus we call this the RBD/2D+slab model. Continuing with the derivation of $\langle \Delta x^2 \rangle$, we express the 2D correlation function $R_{xx}^{2D}(\mathbf{x}_\perp)$ in terms of its Fourier transform, the power spectrum $P_{xx}^{2D}(k_x, k_y)$:

$$R_{xx}^{2D}(\mathbf{x}_\perp) = \frac{1}{2\pi} \int_{-\infty}^{\infty} \int_{-\infty}^{\infty} P_{xx}^{2D}(k_x, k_y) e^{-ik_x x} e^{-ik_y y} dk_x dk_y. \tag{37}$$

Combining Equations (25) and (27) for the 2D contribution, we obtain

$$\begin{aligned} \langle \Delta x^2 \rangle_{2D} = {} & \frac{1}{2\pi} \frac{\Delta z}{B_0^2} \int_{-\infty}^{\infty} \int_{-\infty}^{\infty} P_{xx}^{2D}(k_x, k_y) \\ & \times \int_{-\infty}^{\infty} \left(\int_{-\infty}^{\infty} e^{-ik_x x} P(x|z) dx \right) \\ & \times \left(\int_{-\infty}^{\infty} e^{-ik_y y} P(y|z) dy \right) dz dk_x dk_y, \end{aligned} \tag{38}$$

and specifying the conditional probabilities as Gaussian (Equation (31)) with random ballistic spreading (Equation (36)), we obtain

$$\begin{aligned} \int_{-\infty}^{\infty} e^{-ik_x x} P(x|z) dx &= \exp\left(-\frac{1}{2} k_x^2 \sigma_x^2 \right) \\ &= \exp\left(-\frac{1}{2} \frac{\langle b_x^2 \rangle}{B_0^2} k_x^2 z^2 \right). \end{aligned} \tag{39}$$

Using the analogous result for the integral over y, and using $k_\perp^2 \equiv k_x^2 + k_y^2$, the integral over z in Equation (38) becomes

$$\int_{-\infty}^{\infty} \exp\left(-\frac{1}{2} \frac{\langle b_x^2 \rangle}{B_0^2} k_\perp^2 z^2 \right) dz = \sqrt{\frac{2\pi B_0^2}{\langle b_x^2 \rangle}} \frac{1}{k_\perp} \tag{40}$$

and now we have

$$\begin{aligned} D_\perp^{2D} &= \frac{\langle \Delta x^2 \rangle_{2D}}{2\Delta z} \\ &= \sqrt{\frac{\pi}{2}} \frac{1}{B_0 \sqrt{\langle b_x^2 \rangle}} \frac{1}{2\pi} \int_{-\infty}^{\infty} \int_{-\infty}^{\infty} \frac{P_{xx}^{2D}(k_x, k_y)}{k_\perp} dk_x dk_y \\ &= \frac{\sqrt{\pi}}{2} \frac{1}{B_0 b} \frac{1}{2\pi} \int_{-\infty}^{\infty} \int_{-\infty}^{\infty} \frac{P^{2D}(k_x, k_y)}{k_\perp} dk_x dk_y, \end{aligned} \tag{41}$$

where we use the trace of the spectral matrix, $P^{2D} \equiv P_{xx}^{2D} + P_{yy}^{2D}$.

Next we make use of the total correlation length of the 2D fluctuations, λ_{c2} (Matthaeus et al. 2007), which is the correlation length of P^{2D}. In our notation, λ_{c2} is given by

$$b_{2D}^2 \lambda_{c2} = \frac{1}{2\pi} \int_{-\infty}^{\infty} \int_{-\infty}^{\infty} \frac{P^{2D}(k_x, k_y)}{k_\perp} dk_x dk_y. \tag{42}$$

From this we obtain

$$D_\perp^{2D} = \frac{\sqrt{\pi}}{2} \frac{b_{2D}^2}{B_0 b} \lambda_{c2} = \frac{\sqrt{\pi}}{2} (1 - f_s) \frac{b}{B_0} \lambda_{c2}. \tag{43}$$

This has the noteworthy property of scaling as b/B_0, representing Bohm diffusion. This demonstrates an alternative path to Bohm diffusion, which is novel in the present context, although anticipated to some degree by Kadomtsev & Pogutse (1979). Recall that a heuristic argument for this functional dependence was provided in Section 2.2.

In contrast with the calculation for DD, for RBD there is no implicit dependence of $D_\perp^{2D}$ on $D_\perp$. Therefore, the quasilinear slab contribution and Bohm 2D contribution combine in a direct sum (see also Section 2.2):

$$D_\perp = D_\perp^{slab} + D_\perp^{2D}. \tag{44}$$

Another difference is the characteristic length scale: RBD results in a diffusion coefficient that depends on the total correlation length (i.e., the $k_\perp^{-1}$ moment of the 2D power spectrum), whereas for DD it involves the ultrascale (based on the $k_\perp^{-2}$ moment).

A similar calculation can be performed for a weak (but not very weak) slab contribution, which is the third regime described in Section 2.2. Here we employ RBD, but consider that the slab contribution is diffusive and makes little contribution. Thus, we use the RBD/2D model, and Equation (36) is modified to use the 2D field instead of the sum of 2D+slab fields:

$$\sigma_x^2 = \sigma_y^2 = \frac{\langle b_x^2 \rangle^{2D}}{B_0^2} z^2. \tag{45}$$

This change propagates to change $b \to b_{2D}$ in Equation (43), so we obtain

$$D_\perp^{2D} = \frac{\sqrt{\pi}}{2} \frac{b_{2D}}{B_0} \lambda_{c2} = \frac{\sqrt{\pi}}{2} \sqrt{1 - f_s} \frac{b}{B_0} \lambda_{c2}. \tag{46}$$

This again represents Bohm diffusion, in analogy with Equation (43). This then directly sums with the quasilinear slab contribution,

$$D_\perp = D_\perp^{slab} + D_\perp^{2D}, \tag{47}$$

to yield a novel route to Bohm diffusion.

3. COMPUTER SIMULATIONS

3.1. Techniques

Computer simulations were also used to analyze the diffusion coefficient in 2D+slab turbulence. Because they do not rely on assumptions of the analytic calculation such as Corrsin's hypothesis, Gaussian displacement distributions, DD, or RBD, they provide an independent check of the validity of the analytic calculations. The simulations involved two steps.

1. Generating representations of axisymmetric slab and 2D magnetic fields with desired statistical properties by

means of inverse fast Fourier transforms from **k**-space representations.

2. Tracing the magnetic field lines by solving the coupled ordinary differential Equations (3) using a fourth-order Runge–Kutta method with an adaptive step size regulated by a fifth-order error estimate step (Press et al. 1992).

To generate representations of the slab and 2D magnetic fields, we first set the desired power spectrum for each component. For slab fluctuations, we used

$$P_{xx}^{\rm slab}(k_z) = P_{yy}^{\rm slab}(k_z) = \frac{C^{\rm slab}}{[1+(k_z\lambda)^2]^{5/6}}, \quad (48)$$

where $C^{\rm slab}$ is a normalization constant, set so as to obtain the desired slab turbulence energy $\langle b^2\rangle^{\rm slab} = f_s b^2$, and λ is a parallel coherence scale that is directly related to the correlation length ℓ_c. This spectral form is constant in an energy-containing range at low k_z and follows a Kolmogorov power law ($P_{xx} \propto k_z^{-5/3}$) for turbulence in the inertial range, much like observed fluctuations in the solar wind (e.g., Jokipii & Coleman 1968; Bieber et al. 1996). Our simulations have insufficient dynamic range to model a dissipation range at higher k_z, and in any case we will make comparisons with "discrete theory" formulae for the actual power spectra and **k** values used in the simulations, so as to test whether the theory correctly specifies the influence of each Fourier mode on the field line diffusion (see also Ruffolo et al. 2006). The power spectrum P_{ii} for $i = x, y$ is proportional to the squared Fourier amplitude, $|b_i(k_z)|$, so we derive $b_i(k_z)$ from the square root of the power spectrum times $\exp[i\varphi_i(k_z)]$, where each random phase φ_i for each discrete Fourier mode is independent. The slab magnetic fields in real space are derived from one-dimensional (1D) inverse fast Fourier transforms.

For 2D fluctuations, note that $b_x^{\rm 2D}$ and $b_y^{\rm 2D}$ are not independent. Both are related to the potential function by $\mathbf{b} = \nabla \times [a(x, y)\hat{\mathbf{z}}]$. For the magnetic power spectra in **k**-space, this implies that

$$P_{xx} = k_y^2 A(k_\perp) \qquad P_{yy} = k_x^2 A(k_\perp), \quad (49)$$

where $A(k_\perp)$ is the axisymmetric power spectrum for the potential function $a(x, y)$. The function of A that we use is

$$A(k_\perp) = \frac{C^{\rm 2D}}{[1+(k_\perp\lambda_\perp)^2]^{7/3}}. \quad (50)$$

Here $C^{\rm 2D}$ is set to obtain the desired 2D turbulence energy $\langle b^2\rangle^{\rm 2D} = (1-f_s)b^2$, and $\lambda_\perp$ is a perpendicular coherence scale. Note that the omnidirectional power spectrum, a quantity of relevance to turbulence theory, is a spectral density in terms of the magnitude of **k**. For the 2D component, we have $\mathcal{E}(k_\perp) \sim k_\perp(P_{xx} + P_{yy}) = k_\perp^3 A(k_\perp)$ (see also Ruffolo et al. 2004; Matthaeus et al. 2007), and Equation (50) provides a Kolmogorov power law for the omnidirectional power spectrum in the inertial range. Note also that the power spectra have a $k_\perp^2$-dependence in the energy-containing range as required for homogeneity, and they give rise to a finite ultrascale $\tilde{\lambda}$ of order $\ell_\perp$ (Matthaeus et al. 2007). For each mode in our discrete 2D Fourier space, we derive $a(\mathbf{k})$ from $\sqrt{A(k_\perp)}$ times $\exp[i\varphi(\mathbf{k})]$ for an independent random phase φ. We then derive the components $b_i(\mathbf{k})$ and perform 2D inverse Fourier transforms to obtain $b_i(x, y)$. When summed, the 2D+slab fields vary in all three dimensions, yet each component only requires a 1D or a 2D transform, which is computationally much less expensive than the corresponding three-dimensional transform. This is a major advantage of the 2D+slab magnetic field model.

In the computer code, we set $\lambda = \lambda_\perp = 1$. Therefore, the diffusion coefficients D that we present are also the scaled diffusion coefficients $D' = D(\lambda/\lambda_\perp^2)$ that depend only on r and f_s (see Section 2.2). To obtain D for other λ and $\lambda_\perp$, our reported value serves as D' for the desired values of r and f_s, from which one can obtain $D = D'(\lambda_\perp^2/\lambda)$. We generate slab fields over a periodic box of length $L_z = 100{,}000$ with $N_z = 2^{22} = 4{,}194{,}304$ grid points and 2D fields over $L_x = L_y = 100$ with $N_x = N_y = 4096$ points.

We traced each magnetic field line, i.e., solved the coupled ordinary differential Equations (3), up to $z = 2500$, which is 2.5% of the box length. For each value of r and f_s, we traced 1000 field lines. For these the slab representation was kept fixed, but each field line was started at a random z location along the periodic box. After every 10 field lines, a new 2D representation was generated, to help ensure sufficient sampling of the possible variety of 2D topologies. The initial location of each field line was also random in the x- and y-directions. After tracing these 1000 field lines, another program examined pairs of z values separated by Δz along the same field line, and combined data for all field lines to obtain the mean squared perpendicular displacements $\langle\Delta x^2\rangle$ and $\langle\Delta y^2\rangle$, as well as $D_x = \langle\Delta x^2\rangle/(2\Delta z)$ and $D_y = \langle\Delta y^2\rangle/(2\Delta z)$, for each parallel displacement Δz. For lower Δz values, more samples are available and this implies better statistics for the results. Examples of diffusion coefficients are shown in Figure 3.

In Figure 3, the diffusion coefficient initially rises at low Δz. This is due to the free-streaming regime, where field lines have not yet decorrelated from their initial trajectory. One technical point is that our formulae for D_i are in essence averages of a running diffusion coefficient $\tilde{D}_i = (1/2)(d\langle\Delta x^2\rangle/dz)$ from 0 to Δz. Such averaging provides better statistics, but it allows the free-streaming regime to influence the values D_i over displacements Δz much longer than the coherence length λ. Another technical point is that in Figure 3(a), the values of D_i are seen to slightly decrease over Δz from 500 to 1000. This is due to a periodicity effect. Unlike higher-dimensional fields, the slab field varies only along z and therefore exactly repeats after $\Delta z = L_z = 10^5$. For pure slab turbulence, a perpendicular mean squared displacement such as Δx^2 returns to zero at $\Delta z = L_z$, and indeed takes the form $\Delta x^2 \propto |\sin(\pi\Delta z/L_z)|$ (Chuychai 2005). Such effects are present even when adding a 2D field component. Thus, Figure 3(a) is interpreted as showing free streaming followed by asymptotic diffusion, with values of D_i that decrease slightly as Δz increases above 500 due to the slab periodicity effect.

To determine diffusion coefficients $D_\perp \equiv (D_x + D_y)/2$ from data such as those in Figure 3, we evaluate the following: $D_{\perp p}$, the peak value over $\Delta z = 0$–500, $D_{\perp 1}$, a weighted average over $\Delta z = 500$–1000, and $D_{\perp 2}$, a weighted average over $\Delta z = 1200$–2499. We also report the analogous quantities D_{x1} and D_{y1}. The weight was proportional to $z_{\rm max} - \Delta z$, where $z_{\rm max}$ is the maximum value of Δz used in the averaging. This puts more weight on lower Δz values, which have better statistics because more pairs of points are available for smaller displacements. The diffusion coefficients we report from simulation results are "average 1" values ($D_{\perp 1}$, D_{x1}, or D_{y1}) except where noted. In most cases this range of Δz values is high enough to measure asymptotic diffusion and low enough to avoid strong slab periodicity effects.

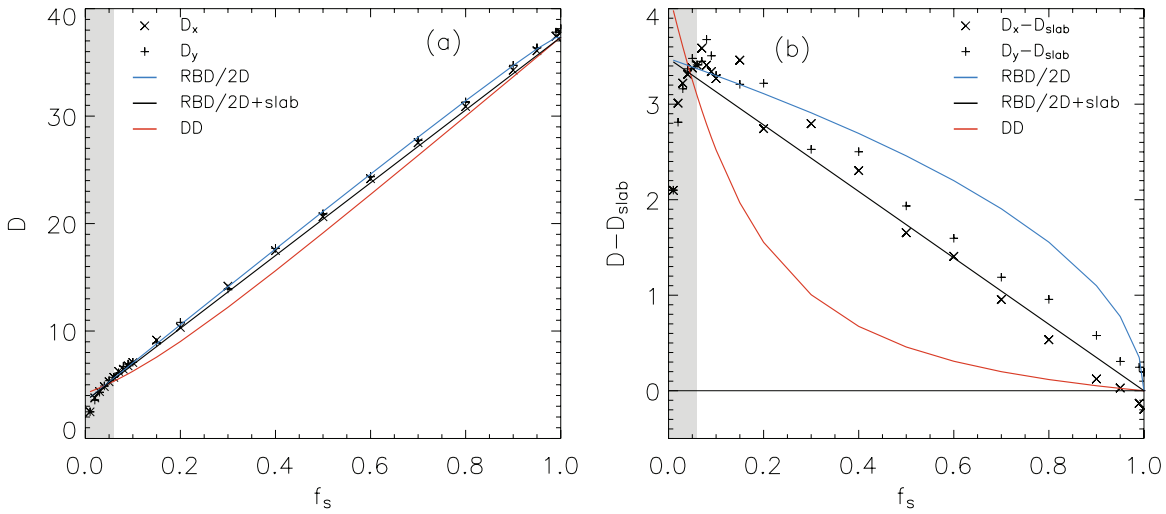

Figure 4. Magnetic field line diffusion coefficients as a function of the slab fraction f_s for a scaled fluctuation amplitude $r = 10$ (i.e., $b/B_0 = 10$), (a) overall and (b) subtracting the slab contribution in order to determine the 2D contribution. Computer simulation results (symbols) and models of Bohm diffusion (lines) are shown. In this case there is a strong slab contribution, and RBD/2D+slab (see Figure 2(a)) can accurately model the 2D contribution, except at very low f_s, where the diffusion coefficient is suppressed due to trapping effects (shaded region).

Figure 3(b) shows a case where subdiffusion is evident from the peak in D_i followed by a concave decrease. At $\Delta z > 500$ the diffusion coefficient appears to decrease, but this may be due to the periodicity effect described above. Therefore, in the present work we simply report whether there is evidence for some subdiffusion and do not attempt to determine whether the asymptotic behavior is diffusive or subdiffusive.

Another technical concern for a very low slab fraction f_s is that field lines may be nearly confined to 2D flux surfaces (i.e., these surfaces are nearly undisturbed), and there is an artifact of the simulations that some 2D equipotential contours and flux surfaces span the periodic box and therefore have infinite extent in x or y, whereas they would be closed structures if the periodic box were larger (or non-existent in the case of an astrophysical plasma). We tried different perpendicular box lengths for $r = 0.1$, the case that should be the most sensitive to such effects, and concluded that the results are reasonably independent of the perpendicular box length so long as $f_s \geqslant 0.01$. We therefore do not examine the FLRW for $f_s < 0.01$ in the present work.

3.2. Results

We examine the validity of quasilinear diffusion, various routes to Bohm diffusion, and trapping effects in the FLRW for 2D+slab turbulence by performing computer simulations for many values of the scaled fluctuation amplitude $r = (b/B_0)(\lambda/\lambda_\perp)$ and the slab fraction $f_s = b_{\rm slab}^2/b^2$. Note that for a given value of f_s, the parameter r is proportional to $D_\perp^{\rm slab}/D_\perp^{\rm 2D}$. Thus, our choice of r sets the relative strength of the slab contribution, and we use the f_s-dependence to distinguish between the three types of Bohm diffusion: DD (Matthaeus et al. 1995), random ballistic diffusion with 2D and slab contributions (RBD/2D+slab), and random ballistic diffusion with a 2D contribution only (RBD/2D). Note also that the results shown here are for $\lambda = \lambda_\perp = 1$, so r is numerically equal to b/B_0. Given our assumption of axisymmetry, our results for D_x and D_y represent independent determinations of $D_\perp$, and their difference indicates the statistical uncertainty of our simulation results. For all models we show the predictions of discrete theory, in which integrals over **k**-space are replaced by discrete sums over the Fourier modes used in the simulations, so as to reduce discretization error and more accurately test the theories.

Figure 4 shows results for $r = 10$, where the slab contribution is typically strong. Recall that the slab contribution is quasilinear, with $D_\perp^{\rm slab} \propto f_s$ (Equation (30)), and indeed the overall diffusion coefficient $D_\perp$ is dominated by such a trend (Figure 4(a)). The three models of Bohm diffusion yield only minor differences in $D_\perp$, but the ~1% precision of our results is sufficient to distinguish between them.

To more clearly compare the simulation results with the three models of Bohm diffusion for the 2D contribution, in Figure 4(b) we subtract out the slab contribution. The slab contribution is generally accepted to be quasilinear and hence proportional to f_s, so we can subtract it to show $D_\perp - D_\perp^{\rm slab}$ for each of the models. For simulation results, we subtract f_s times the value of $D_\perp = (D_x + D_y)/2$ for pure slab fluctuations ($f_s = 1$). The simulation results agree very well with the RBD/2D+slab model of the 2D contribution, as expected in Section 2 for the case of a strong slab contribution. The agreement is clearly better than for the RBD/2D or DD model. Note that the DD model for $D_\perp - D_\perp^{\rm slab}$ is concave in Figure 4(b) because of the special quadratic addition of $D_\perp^{\rm 2D}$ with $D_\perp^{\rm slab}$ (Equation (34)). The other two models use a direct sum, so $D_\perp - D_\perp^{\rm slab}$ is simply $D_\perp^{\rm 2D}$.

For low slab fractions, the field line diffusion coefficient drops sharply compared with the models. This is true for every r value we studied (see Figures 4–7), indicating that some other factors besides the Bohm diffusion need to be taken into account. The decrease in $D_\perp$ can be attributed to trapping effects, as we shall discuss shortly.

Figure 5 shows results for $r = 1$. For $f_s > 0.1$, both DD and RBD/2D provide rough approximations to $D_\perp$, but with errors of ~10% and somewhat inaccurate representations of the f_s-dependence. These ambiguous results could be attributed to a transition between routes to Bohm diffusion as the slab contribution varies with f_s.

Results for $r = 0.3$ are shown in Figure 6. Here the simulation results are best explained in terms of a 2D contribution given by the DD model with trapping effects at low f_s. This is consistent with the expectation that DD should be valid for a moderate slab contribution.

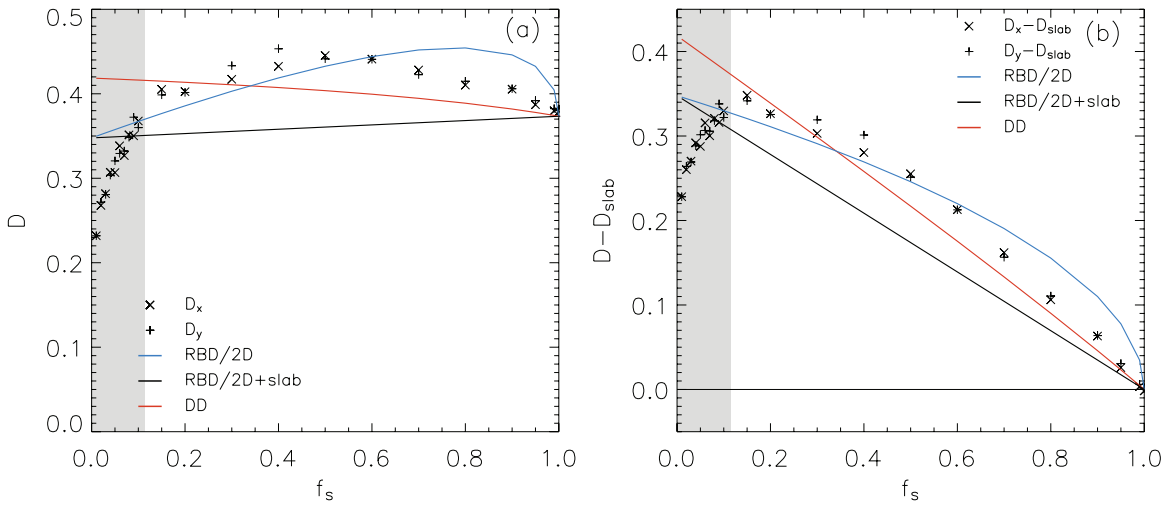

Figure 5. Like Figure 4, but for $r = 1$. In this intermediate regime, two models of Bohm diffusion (DD and RBD/2D) can roughly describe the 2D contribution, except at very low f_s where trapping effects are evident (shaded region).

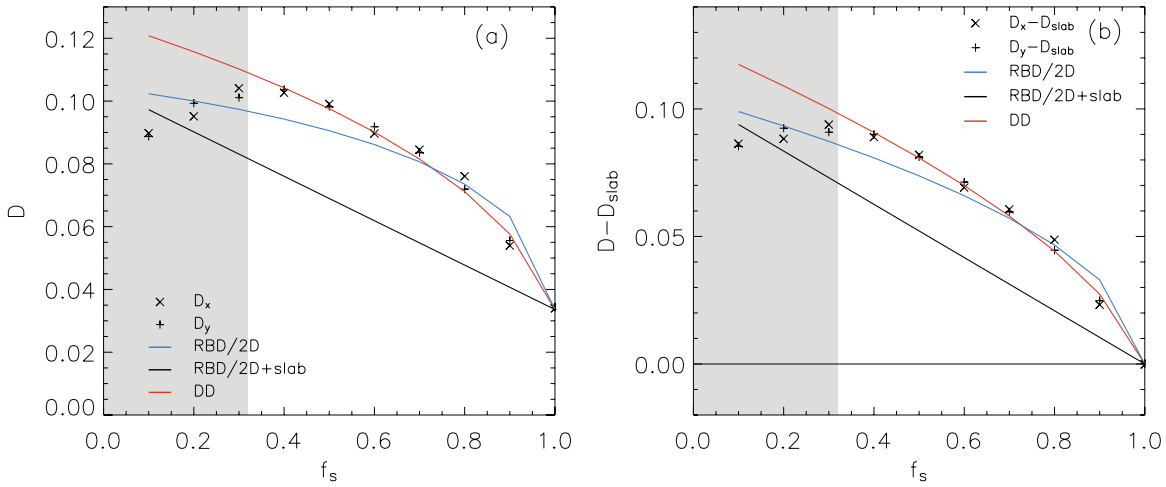

Figure 6. Like Figure 4, but for $r = 0.3$. Here there is a moderate slab contribution, and DD as in Matthaeus et al. (1995) (see Figure 2(b)) can explain the 2D contribution, except at low f_s where trapping effects are evident (shaded region).

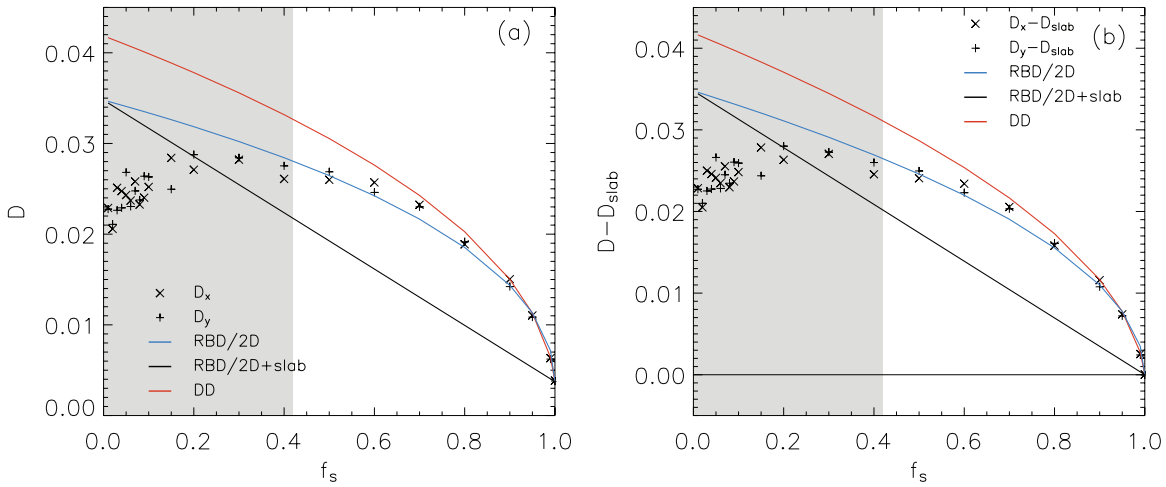

Figure 7. Like Figure 4, but for $r = 0.1$. Here there is a weak slab contribution, and RBD/2D (see Figure 2(c)) can accurately model the 2D contribution, except at low f_s where trapping effects are evident (shaded region). Note that at high f_s, DD can also model the 2D contribution.

Figure 7 shows our results for $r = 0.1$. Note that for this figure we display values of D_{x2} and D_{y2} (weighted averages over $\Delta z = 1200$–2499) because in some cases the influence of the free-streaming regime persisted during our usual averaging interval for D_{x1} and D_{y1} (the interval of $\Delta z = 500$–1000). Again there are trapping effects for low f_s, and for moderate to high f_s the simulation data are best explained in terms of the RBD/2D model, as expected for the low slab contribution at such a low

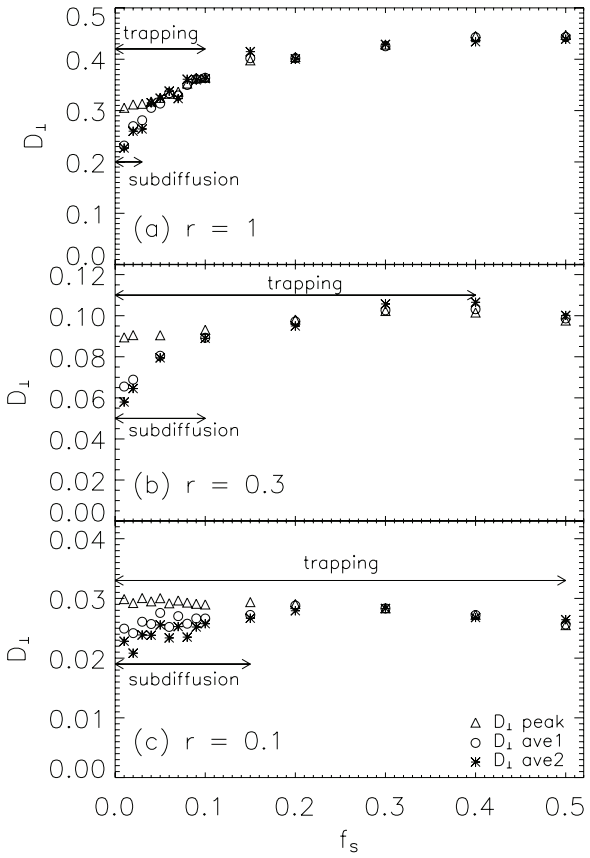

Figure 8. Magnetic field line diffusion coefficients $D_\perp$ from computer simulations as a function of the slab fraction f_s for (a) $r = 1$, (b) $r = 0.3$, and (c) $r = 0.1$. Trapping effects for very low slab contributions (see Figure 2(d)) are identified in terms of deviations from the high-f_s trends in Figures 5–7. Symbols represent $D_{\perp p}$ (triangles), $D_{\perp 1}$ (circles), and $D_{\perp 2}$ (asterisks) for increasing z-ranges as defined in the text. Subdiffusion is identified from a systematic decrease in $D_\perp$ values for increasing z. While trapping effects are limited to low f_s values, subdiffusion is limited to even lower f_s.

value of r (see Section 2). Note that the DD model also matches the simulation results at high f_s.

Results for $f_s \leqslant 0.5$ are shown in Figure 8 for various values of r, in order to further examine the trapping effects. For one thing, we note that the decreases in $D_\perp$ imply changes in the 2D contribution to field line diffusion, because at very low f_s values the slab contribution is so small that its complete removal could not explain the decrease. The arrows that indicate trapping in this figure give only a rough indication of the range in f_s where trapping effects apparently cause a reduction in $D_\perp$ below the appropriate model trend. For example, for $r = 0.3$ the decline in $D_\perp$ at low f_s could be partially due to a transition between routes to Bohm diffusion (from DD to RBD/2D). However, while trapping effects are evident, as anticipated in many previous studies (see Section 1), the simulation results remain within a factor of two of all models of Bohm diffusion.

While trapping effects are indicated by a reduction in $D_\perp$ at low f_s values, they cause subdiffusion only at an even lower range in f_s. This can be seen in Figure 8, where different symbols indicate simulation results for $D_\perp$ in different ranges of Δz (as specified in Section 3.1). Arrows indicate ranges of f_s where subdiffusion is manifest as a systematic decrease in $D_\perp$ values for increasing Δz-ranges.

4. DISCUSSION AND CONCLUSIONS

A high level of precision has been achieved in performing simulations of the magnetic FLRW for disturbed flux surfaces. For a wide range of parameter values, good agreement can be obtained with the appropriate model. Such precision is obtained in part because we typically use results for $\Delta z < 0.01 L_z$ in order to avoid slab periodicity effects. In this work we point out that there are multiple routes to Bohm diffusion and present analytic theories for these, and the precision of the simulation results is the key to distinguishing among them.

This work employed the 2D+slab model of magnetic turbulence, which has provided a useful description of turbulence in the interplanetary medium. We have employed random-phase models of the slab and 2D turbulence components. Some recent studies of the spatial patterns of turbulent FLRWs have employed a more physical 2D MHD model of the 2D component (Kittinaradorn et al. 2009; Seripienlert et al. 2010). We therefore performed simulations to check the difference between $D_\perp$ for a 2D random-phase field and a 2D MHD field. The latter type of field is more difficult to generate and therefore we had a smaller sample size and encountered a larger statistical uncertainty. Within such uncertainty, we found no difference between $D_\perp$ for the two types of fields. This may be because the 2D contribution involves an integral of the power spectrum with a weighting of $k_\perp^{-1}$ or $k_\perp^{-2}$, and the low-$k_\perp$ modes are relatively unchanged by the 2D MHD dynamics (Seripienlert et al. 2010). Therefore, we conclude that random-phase fields seem to be sufficiently accurate for computer simulations of $D_\perp$.

Trapping effects are clearly evident at a low slab fraction, f_s, and the FLRW exhibits subdiffusion at even lower f_s. The trapping phenomenon was anticipated in numerous theoretical studies for the nearly 2D limit (see Section 1), and indicates at least a partial failure of the assumptions underlying our theories of Bohm diffusion in these parameter ranges. Because of subdiffusion, we do not obtain a well-defined diffusion coefficient for nearly 2D fluctuations, making it difficult to compare our simulation results with specific predictions for $D_\perp$ from percolation theory. Indeed, subdiffusion was not addressed in classical percolation models, though it has been seen in previous numerical results in the nearly 2D limit for the FLRW (Ruffolo et al. 2008) and for related problems (e.g., Ottaviani 1992).

A question that frequently arises in the literature is: when is Corrsin's hypothesis valid? (For some general considerations, see Weinstock 1976.) In the context of our work, one can pose three related questions. (1) Is there a substantial violation of independence between $b_x(0,0)b_x(\mathbf{x}_\perp, z)$ and $P(\mathbf{x}_\perp|z)$? (See Section 2.3.) (2) Given a violation of independence, is there a non-negligible error of approximation in Corrsin's hypothesis? (3) Given an error in Corrsin's hypothesis, is there a significant effect on the integral over the Lagrangian correlation to obtain a running or asymptotic diffusion coefficient?

In some cases we can answer question (1). A memory effect is likely to produce a violation of independence. Since subdiffusion implies a negative Lagrangian correlation and hence a negative memory effect (see also Ruffolo et al. 2008), a subdiffusive regime does indicate a violation of independence. Furthermore, we are convinced that independence is always violated for very short distances z, in the free-streaming regime. However, it is not obvious whether or when this implies an error in Corrsin's hypothesis or an effect on the diffusion coefficient (especially for large Δz). To address questions (2)

and (3), we must note that our analytic derivations introduce two additional assumptions: setting $P(\mathbf{x}_\perp|z)$ to be Gaussian and specifying a functional form for the mean squared displacement. For the numerous cases when a combination of quasilinear and Bohm diffusion can match the simulation results for the FLRW diffusion coefficient, we can answer (3) and infer no significant effects of the violation of Corrsin's hypothesis. When there is a significant difference from the simulation results (especially for low slab fractions), we cannot necessarily infer a violation of Corrsin's hypothesis or effects thereof, because there may also be difficulties with the other assumptions of the theory.

Indeed, the present work stresses the importance of the assumption of a particular physical process leading to decorrelation. This leads to adoption of a functional form for the mean squared displacement in $P(\mathbf{x}_\perp|z)$. One of the concrete results of the present paper is that while DD may be responsible for the diffusive FLRW under some conditions, the random free streaming seems to be responsible under other conditions. Hence there are multiple routes to Bohm diffusion. In actuality, there should be a transition from free streaming to diffusion, so RBD and DD represent limiting behaviors. Further work to investigate such a transition could clarify the range of applicability of each diffusion model.

It is interesting to note that our functional form for $D_\perp^{2D}$ with Bohm diffusion due to RBD (Equation (43) or (46)) can also be obtained using a non-Gaussian probability distribution $P(\mathbf{x}_\perp|z)$. Inspired by the delta-function form of Webb et al. (2006), with a single velocity used to treat the ballistic transport of a distribution of particles, we have repeated the calculations of Section 2.3 using $P(\mathbf{x}_\perp|z) = \delta[x - (b/B_0)z]\delta(y)$. We obtain the same results as in Equations (43) and (46), except that the prefactor is lower by $\sqrt{\pi}$. This model employs a specific value of $\mathbf{b}$ at low z, $\mathbf{b} = b\hat{\mathbf{x}}$ (which indeed could be rotated throughout the x–y plane), before randomization of the field at greater z. The resulting diffusion model could be called ballistic diffusion (as opposed to *random* ballistic diffusion). While one does not normally expect such a "prepared" initial condition in an astrophysical plasma, and with the reduced prefactor the model evidently does not match our computer simulations in which $\mathbf{b}$ has a Gaussian distribution, it does demonstrate that this form of Bohm diffusion does not rely on the assumption of a Gaussian probability distribution.

In this work, we have concentrated on relatively small differences between models of the field line diffusion coefficient in 2D+slab turbulence. Thus, it is important to consider that in a broad perspective, all three models of Bohm diffusion for the 2D contribution, combined with quasilinear diffusion for the slab contribution, can explain all our simulation data to within a factor of two (spanning over three orders of magnitude in $D_\perp$, two orders in f_s, and two orders in r). While trapping effects and subdiffusion are sometimes seen in the simulation results, and there is room for further model development concerning such effects as well as the transition between routes to Bohm diffusion, the strong rejection of Bohm diffusion by some previous authors would seem to be inappropriate, at least based on this extensive set of simulations for 2D+slab fluctuations.

It is interesting to compare the FLRW for the two-component 2D+slab model of magnetic turbulence, as examined here, with results from a one-component model of isotropic turbulence that is stretched (or squashed) in $\mathbf{k}$-space, as simulated in the recent work by Hauff et al. (2010). That work examined the FLRW by means of particles that followed field lines with little pitch angle scattering. According to that work, when a 2D structure "decays" as a function of z, a previously trapped field line becomes open. However, according to Chuychai et al. (2007), in 2D+slab turbulence the slab field can always carry some field lines out of a 2D structure, without requiring the structure to "decay." This might be a reason why Zimbardo et al. (2000) and Hauff et al. (2010) did not find a clear regime of Bohm diffusion during their reported transition in the FLRW from quasilinear to percolative behavior.

In conclusion, we have examined a magnetic fluctuation model in which the random walk of field lines exhibits quasilinear diffusion, Bohm diffusion, and trapping effects over various parameter ranges, showing that these behaviors are not mutually exclusive. Trapping effects, and sometimes even subdiffusion, are found in the limit where the FLRW is largely constrained to only weakly disturbed 2D flux surfaces. In addition to a previously described route to Bohm diffusion based on DD (Matthaeus et al. 1995), we have developed variant analytic theories for additional routes to Bohm diffusion involving RBD. Computer simulations verify that each type of Bohm diffusion provides a useful description of field line diffusion over a different parameter range.

This work was partially supported by a Postdoctoral Fellowship from Mahidol University, the Thailand Research Fund, NSF grant AGS-1063439, NSF SHINE grant ATM-0752135, and NASA grant NNX-09AG31G. D.R. thanks the Department of Physics and Astronomy, University of Delaware for their kind hospitality while part of this work was carried out. The authors thank the anonymous referee for useful suggestions.

REFERENCES

Belcher, J. W., & Davis, L., Jr. 1971, J. Geophys. Res., 76, 3534
Bieber, J. W., Matthaeus, W. H., Shalchi, A., & Qin, G. 2004, Geophys. Res. Lett., 31, L10805
Bieber, J. W., Matthaeus, W. H., Smith, C. W., et al. 1994, ApJ, 420, 294
Bieber, J. W., Wanner, W., & Matthaeus, W. H. 1996, J. Geophys. Res., 101, 2511
Carbone, V., Malara, F., & Veltri, P. 1995, J. Geophys. Res., 100, 1763
Cho, J., & Lazarian, A. 2002, Phys. Rev. Lett., 88, 245001
Chuychai, P. 2005, PhD thesis, Chulalongkorn Univ.
Chuychai, P., Ruffolo, D., Matthaeus, W. H., & Meechai, J. 2007, ApJ, 659, 1761
Chuychai, P., Ruffolo, D., Matthaeus, W. H., & Rowlands, G. 2005, ApJ, 633, L49
Corrsin, S. 1959, in Atmospheric Diffusion and Air Pollution, ed. F. Frenkel & P. Sheppard (Advances in Geophysics, Vol. 6; New York: Academic Press), 161
Dasso, S., Milano, L. J., Matthaeus, W. H., & Smith, C. W. 2005, ApJ, 635, L181
Giacalone, J., Jokipii, J. R., & Mazur, J. E. 2000, ApJ, 532, L75
Gosling, J. T., Skoug, R. M., McComas, D. J., & Mazur, J. E. 2004, ApJ, 614, 412
Gray, P. C., Pontius, D. H., Jr., & Matthaeus, W. H. 1996, Geophys. Res. Lett., 23, 965
Green, M. S. 1951, J. Chem. Phys., 19, 1036
Gruzinov, A. V., Isichenko, M. B., & Kalda, Ya. L. 1990, Sov. Phys. JETP, 70, 263
Hauff, T., Jenko, F., Shalchi, A., & Schlickeiser, R. 2010, ApJ, 711, 997
Isichenko, M. B. 1991a, Plasma Phys. Control. Fusion, 33, 795
Isichenko, M. B. 1991b, Plasma Phys. Control. Fusion, 33, 809
Jokipii, J. R. 1966, ApJ, 146, 480
Jokipii, J. R., & Coleman, P. J. 1968, J. Geophys. Res., 73, 5495
Jokipii, J. R., & Parker, E. N. 1968, Phys. Rev. Lett., 21, 44
Kadomtsev, B. B., & Pogutse, O. P. 1979, in Proc. Seventh Int. Conf., Plasma Physics and Controlled Nuclear Fusion Research 1978 (Vienna: IAEA), 649
Kittinaradorn, R., Ruffolo, D., & Matthaeus, W. H. 2009, ApJ, 702, L138
Kubo, R. 1957, J. Phys. Soc. Japan, 12, 570
Kubo, R. 1963, J. Math. Phys., 4, 174

Leamon, R. J., Smith, C. W., Ness, N. F., Matthaeus, W. H., & Wong, H. K. 1998, J. Geophys. Res., 103, 4775
Matthaeus, W. H., Bieber, J. W., Ruffolo, D., Chuychai, P., & Minnie, J. 2007, ApJ, 667, 956
Matthaeus, W. H., & Ghosh, S. 1999, in AIP Conf. Proc. 471, Solar Wind Nine, ed. S. Habbal, R. Esser, J. V. Hollweg, & P. A. Isenberg (Woodbury, NY: AIP), 519
Matthaeus, W. H., Goldstein, M. L., & Roberts, D. A. 1990, J. Geophys. Res., 95, 20673
Matthaeus, W. H., Gray, P. C., Pontius, D. H., Jr., & Bieber, J. W. 1995, Phys. Rev. Lett., 75, 2136
Matthaeus, W. H., Qin, G., Bieber, J. W., & Zank, G. 2003, ApJ, 590, L53
Mazur, J. E., Mason, G. M., Dwyer, J. R., et al. 2000, ApJ, 532, L79
Negrea, M., Petrisor, I., & Weyssow, B. 2007, Plasma Phys. Control. Fusion, 49, 1767
Neuer, M., & Spatschek, K. H. 2006, Phys. Rev. E, 74, 036401
Osman, K. T., & Horbury, T. S. 2007, ApJ, 654, L103
Ottaviani, M. 1992, Europhys. Lett., 20, 111
Pommois, P., Veltri, P., & Zimbardo, G. 2001, Phys. Rev. E, 63, 066405
Pommois, P., Zimbardo, G., & Veltri, P. 2005, Adv. Space Res., 35, 647
Press, W. H., Teukolsky, S. A., Vetterling, W. T., & Flannery, B. P. 1992, Numerical Recipes in FORTRAN: The Art of Scientific Computing (Cambridge: Cambridge Univ. Press)
Reuss, J.-D., & Misguich, J. H. 1996, Phys. Rev. E, 54, 1857
Ruffolo, D., Chuychai, P., & Matthaeus, W. H. 2006, ApJ, 644, 971
Ruffolo, D., Chuychai, P., Wongpan, P., et al. 2008, ApJ, 686, 1231
Ruffolo, D., Matthaeus, W. H., & Chuychai, P. 2003, ApJ, 597, L169
Ruffolo, D., Matthaeus, W. H., & Chuychai, P. 2004, ApJ, 614, 420
Salu, Y., & Montgomery, D. C. 1977, Phys. Fluids, 20, 1
Seripienlert, A., Ruffolo, D., Matthaeus, W. H., & Chuychai, P. 2010, ApJ, 711, 980
Shalchi, A., Bieber, J. W., Matthaeus, W. H., & Schlickeiser, R. 2006, ApJ, 642, 230
Shebalin, J. V., Matthaeus, W. H., & Montgomery, D. 1983, J. Plasma Phys., 29, 525
Smith, C. W., Mullan, D. J., & Ness, N. F. 2004, J. Geophys. Res., 109, A01111
Smith, C. W., Mullan, D. J., Ness, N. F., Skoug, R. M., & Steinberg, J. 2001, J. Geophys. Res., 106, 18625
Taylor, G. I. 1920, Proc. Lond. Math. Soc., 20, 196
Tooprakai, P., Chuychai, P., Minnie, J., et al. 2007, Geophys. Res. Lett., 34, L17105
Urch, I. H. 1977, Ap&SS, 46, 389
Vlad, M., Spineanu, F., Misguich, J. H., & Balescu, R. 1998, Phys. Rev. E, 58, 7359
Webb, G. M., Zank, G. P., Kaghashvili, E. Kh., & le Roux, J. A. 2006, ApJ, 651, 211
Weinhorst, B., Shalchi, A., & Fichtner, H. 2008, ApJ, 677, 671
Weinstock, J. 1976, Phys. Fluids, 19, 1702
Weygand, J. M., Matthaeus, W. H., Dasso, S., et al. 2009, J. Geophys. Res., 114, A07213
Zimbardo, G., Pommois, P., & Veltri, P. 2004, J. Geophys. Res., 109, A02113
Zimbardo, G., Veltri, P., & Pommois, P. 2000, Phys. Rev. E, 61, 1940